RC23232 (W0406-026) June 8, 2004
Chemistry

IBM Research Report

Chemical Etching of MRAM Permalloy Soft Layers: Role of Passive Films

E. J. O'Sullivan, D. W. Abraham, A. G. Schrott
IBM Research Division
Thomas J. Watson Research Center
P.O. Box 218
Yorktown Heights, NY 10598

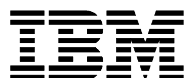

Research Division
Almaden - Austin - Beijing - Haifa - India - T. J. Watson - Tokyo - Zurich

LIMITED DISTRIBUTION NOTICE: This report has been submitted for publication outside of IBM and will probably be copyrighted if accepted for publication. It has been issued as a Research Report for early dissemination of its contents. In view of the transfer of copyright to the outside publisher, its distribution outside of IBM prior to publication should be limited to peer communications and specific requests. After outside publication, requests should be filled only by reprints or legally obtained copies of the article (e.g., payment of royalties). Copies may be requested from IBM T. J. Watson Research Center, P. O. Box 218, Yorktown Heights, NY 10598 USA (email: reports@us.ibm.com). Some reports are available on the internet at http://domino.watson.ibm.com/library/CyberDig.nsf/home.

CHEMICAL ETCHING OF MRAM PERMALLOY SOFT LAYERS: ROLE OF PASSIVE FILMS

E. J. O'Sullivan, D.W. Abraham, and A.G. Schrott
IBM Research Division
Thomas J. Watson Research Center
P.O. Box 218
Yorktown Hts., NY 10598, USA

ABSTRACT

Chemical etching was used for selective patterning of magnetic soft (or free) layers, principally Permalloy, in MRAM stacks. Passive films formed in the prior cap layer patterning step played a critical role in the etching behavior of the magnetic layers. The novel use of a sulfur-based additive to inhibit Permalloy passivation, thus enabling selective etching in weak acid etchants, was demonstrated. Aqueous etch solutions of α, ω-dicarboxylic acids were found to etch Permalloy films whose surfaces contained a chemisorbed, sulfur-based, passivation inhibitor, but left the alumina tunnel barrier intact. High values of array quality factors for magnetic switching were demonstrated for chemically etched arrays of Permalloy elements.

INTRODUCTION

Magnetic tunnel junctions (MTJ) show much promise for magnetic random access memory (MRAM) (1-3). This is principally due to nonvolatility (memory retention without power consumption), high read and write cycles of a few nanoseconds duration, and eventually high memory density (bits per unit area) approaching that of dynamic random access memory (DRAM).

MTJ stacks, which are of submicron dimensions, tend be of the form shown in Fig. 1. An adhesion layer (e.g. Ta-based) is first deposited, and followed by an antiferromagnetic layer (e.g. Ir-Mn, Pt-Mn alloys). A fixed-moment magnetic layer (e.g. 15 Å $Co_{90}Fe_{10}$) is followed by a thin Al layer (e.g., 8-16 Å) which is then oxidized to form the AlO_x tunnel barrier. A soft magnetic layer (e.g. 50 Å $Ni_{81}Fe_{19}$) and a protective capping layer (e.g. 100-200 Å Ta-based) complete the stack. Deposition of blanket films is usually carried out by physical vapor deposition methods (PVD) or related methods.

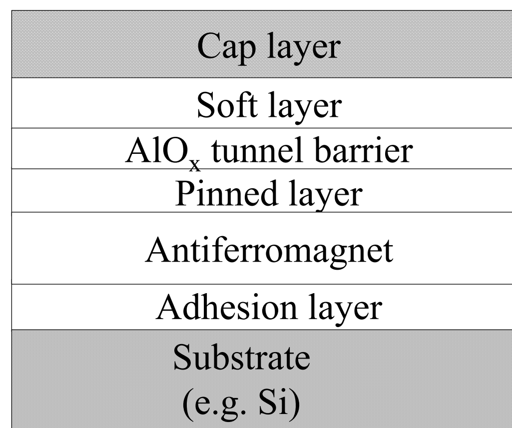

Figure 1. Schematic representation of a magnetic tunnel junction**.**

Figure 2(a) shows schematically the write operation of an MTJ. The moment of the bottom ferromagnetic layer, which is located beneath the tunnel barrier, is immobilized through an "exchange bias" interaction with the antiferromagnetic layer. The moment of the ferromagnetic layer located above the tunnel barrier (known as the "free", or soft, layer), may be oriented either parallel or antiparallel to that of the pinned layer (Fig. 2(b)). The MTJ resistance is typically lower in the former case, enabling two distinct data states, "0" and "1", to be obtained (Fig. 2(c)). Since the tunnel barrier is highly resistive, yet only 1-2 nm in thickness, electrical conduction occurs by quantum mechanical tunneling, and importantly, spin is conserved during the tunneling process in the MTJs.

In the parallel moments case, electrons of a particular spin, say "spin-up" type, are favored by the free layer, and tunnel into the "spin-up" empty states which predominate at the alumina barrier/pinned layer interface. In the antiparallel moments case, "spin-down" electrons are favored in the free layer. These cannot tunnel into the "spin-up" empty states predominating at the alumina barrier/pinned layer interface, but rather tunnel into the less predominant "spin-down" empty states. Typically the magnitude of the resistance difference between both states is ca. 30 – 50 %, which appears to be large enough for practical application (integration with CMOS technology).

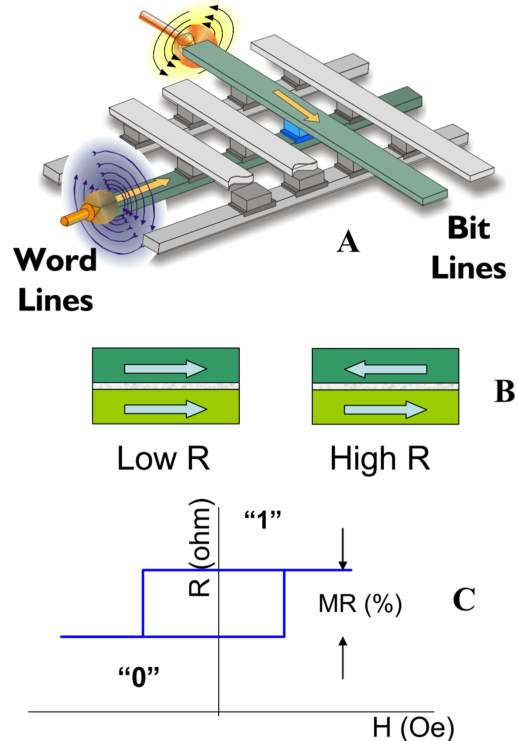

Figure 2. Schematic of MRAM write and read operations.

A practical MRAM chip also has to have a sufficiently tight distribution of switching fields in order to allow selection of a particular bit in the writing process. A useful figure of merit for write yield is the "array quality factor" (AQF), which is defined as the ratio of mean switching field to the standard deviation of the switching field for the tunnel junctions in the MRAM device. Calculations show that write failures will occur if AQF is less than approximately 20. These failures are either half-select errors (flipping occurs when only the word or the bit line field is applied) or full-select errors (flipping does not occur even when both word and bit line fields are applied to the bit). Thus, high AQF is a critical requirement for successful MRAM operation, and is in practice strongly influenced by the quality of the MTJ definition process.

The options for patterning the MRAM stack typically include ion beam etching (IBE), reactive ion etching (RIE), chemical (wet) etching, or a combination of these methods. Each etching method is not without problems. Thus, IBE, being a purely physical etching method, is non-selective, and material redeposition is a major problem. Halogen gas-based RIE methods cleanly chemically etch valve-metal-based layers, such

as Ta, but will not chemically etch Permalloy at significant rates in low-density plasma environments.

The thin film nature of MRAM magnetic films (20-50 Å z-direction) relative to the x-y dimensions of patterned MTJ elements (presently > 1,000-2,000 Å) makes them attractive for chemical etching, since, aside from Galvanically-enhanced dissolution, the isotropic property of chemical etching should not result in excessive lateral etching. However, such thin films require weak etchant solutions in order to minimize lateral etching but enhance etch selectivity, e.g., not etch through the alumina barrier.

This paper describes initial fundamental chemical etching results for Permalloy ($Ni_{81}Fe_{19}$) in MTJ stack and single layer configurations, and the interplay between passivation, resulting from the preceding cap layer patterning step, and film dissolution.

EXPERIMENTAL

All MRAM films were deposited using PVD methods on Si wafers. The alumina tunnel barriers were formed by exposing Al layers to air. Reactive ion etching was carried out in a PlasmaLab µP tool. Mask creation was carried out using either standard photoresist processing methods, or ebeam lithography methods. Reagent grade chemicals and 18 Mega Ohm DI water were employed. Magnetic film etching was confirmed using sheet resistance and vibrating sample magnetometry (VSM) measurements, and X-ray photoelectron spectroscopy (XPS).

RESULTS AND DISCUSSION

Ti-Capped Permalloy Soft Layers

Early MRAM stacks at IBM utilized Ti as a capping layer on the Permalloy soft layer (see Fig. 1). Generally Ti films may be etched or patterned using either fluorine-based RIE or HF-containing solutions. However, etching thin Ti layers (in this case 100 Å thick) in a controlled manner using dilute (e.g. $\leqslant 0.1$ mol dm^{-3}) HF solution was difficult owing to the passive oxide film on the Ti surface which appeared to grow over the course of 24 hr following PVD-type deposition. Thus, chemical etching of thin Ti layers in dilute HF solution was characterized by a variable induction period relating to dissolution of the passive film, followed by rapid dissolution of the unoxidized Ti.

To overcome the inhibiting effect of the Ti passive film, the Ti-capped stacks were first subjected to a CF_4/Ar(10 %) plasma to remove the surface film. Within ca. 2 hours, the remaining Ti was etched in the aqueous solution shown in Table 1. In this solution, the succinic acid and sodium fluoride combined to provide a buffered source of HF to etch Ti. Benzotriazole (BTA) chemisorbed on newly-exposed $Ni_{81}Fe_{19}$ inhibiting its dissolution, thus enabling it to be etched in a solution selective to $Ni_{81}Fe_{19}$. Benzotriazole, which has long been used as a corrosion inhibitor for Cu (where it forms a $(Cu[I]\text{-}BTA)_n$ layer) evidently chemisorbed on the Permalloy surfaces. Complete removal of Ti in the RIE plasma resulted in a passivated $Ni_{81}Fe_{19}$ surface which inhibited etching in solutions

other than those of strong acids or those containing oxidants that promote dissolution rather than passivation.

Table 1: Ti Etching Solution

Succinic acid	0.1 mol dm^{-3}
NaF	0.05 mol dm^{-3}
Benzotriazole	0.1 mol dm^{-3}
Thiourea	10 ppm
pH	4.3
Temperature	25 °C

An objective of the present work was to develop a soft layer etching process that did not etch past the alumina tunnel barrier and etch the $Co_{90}Fe_{10}$ pinned magnetic layer (which is considerably more reactive than Permalloy). This ruled out conventional acid etchants such as sulfuric acid which caused the alumina barrier (bulk alumina is mildly basic with a pH of zero charge (PZC) of ca. 9.0) to etch rapidly, e.g. in ⩽ 1 min in 0.02 mol dm^{-3} H_2SO_4. Thus, attention was turned to aqueous solutions of carboxylic acids, in particular α, ω-dicarboxylic acids, some of which are listed in Table 2. Immersion of the RIE-exposed $Ni_{81}Fe_{19}$ in a dilute solution of dicarboxylic acid, e.g. of concentration 0.01 – 0.1 mol dm^{-3} at pH 4 – 5, resulted in facile dissolution of the $Ni_{81}Fe_{19}$ layer (2 Å/s rate). Thiourea-related species chemisorbed on the $Ni_{81}Fe_{19}$ surface were critical for initiation of $Ni_{81}Fe_{19}$ dissolution in the weak dicarboxylic acid etchant. Throughout this work, the pH of these solutions was maintained in the 4 – 5 range in order to, as much as possible, reduce alumina tunnel barrier dissolution.

Table 2: Etching Solutions: α, ω-dicarboxylic acids, HOOC(CH2)$_n$COOH

Acid	n
Malonic	1
Succinic	2
Glutaric	3
Adipic	4
Glutaric	5
Suberic	6
Azelaic	7

Completion of $Ni_{81}Fe_{19}$ layer etching was confirmed using sheet resistance and vibrating sample magnetometry (VSM) measurements, and X-ray photoelectron spectroscopy (XPS). Following Ti etching, the presence of a distinct, chemisorbed TU-related S species was confirmed by XPS (Fig. 3(a)). This species prevented the formation of a passivating layer on the $Ni_{81}Fe_{19}$ surface during DI water rinsing. In contrast, Permalloy did not etch if TU was omitted from the Ti etch solution (see Fig. 3(b)).

Stopping the etching at the tunnel barrier avoids Galvanic corrosion reactions (due to the reactive fixed moment layer being in contact with noble metal-based AF one). If the alumina tunnel barrier thickness exceeded ≥ 12-15 Å[1], and was well formed (well oxidized, pinhole-free), etch selectivity was such that the more reactive fixed-moment $Co_{90}Fe_{10}$ located beneath the barrier remained intact. This was confirmed by VSM, and XPS. Figure 4 shows XPS data recorded at two different angles following soft layer removal in a suberic acid solution; it shows that the alumina tunnel barrier and the $Co_{90}Fe_{10}$ pinned layer are present . The dicarboxylic acids, $HOOC(CH_2)_nCOOH$, with n = 5 – 7 (Table 2), which do not form stable chelate ring complexes with Al^{+3},

[1] The final thickness of the AlO_x tunnel barrier is implied here, not the original Al thickness.

reacted least with alumina, as compared to, e.g., malonic acid (n = 1), which can form relatively stable 6-membered chelate ring compounds with Al^{+3}. The solubility of these acids in aqueous solution is strongly dependent on the value of "n"; the solubility of azelaic acid is essentially too low for practical use. Suberic acid was the etchant favored in this work.

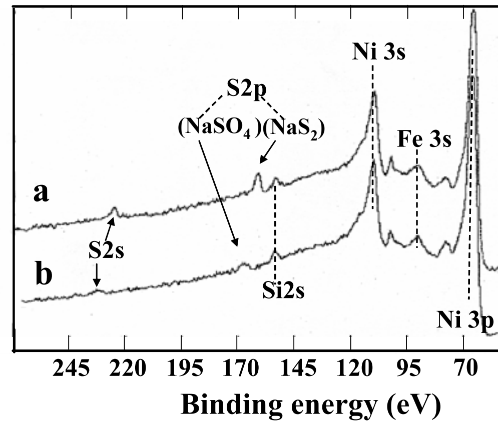

Figure 3. XPS characterization results for a) Permalloy surface after Ti etchant solution + TU, and b) TU-free etchant.

Ta-Capped Permalloy Soft layers

Compared to Ti, Ta cap layers impart improved properties to MRAM stacks, but may only be patterned using a RIE plasma containing reactive halogen species rather than by conventional chemical etching. Magnetic tunnel junction stacks with CF_4/Ar–patterned Ta cap layers did not exhibit $Ni_{81}Fe_{19}$ dissolution in suberic acid etchant. However, the use of SF_6 gas in place of CF_4 during RIE patterning of the Ta resulted in the $Ni_{81}Fe_{19}$ soft layers readily dissolving in the latter solution. X-ray photoelectron spectroscopy confirmed the presence of minute amounts of S on the surface of $Ni_{81}Fe_{19}$ following Ta removal. The chemisorbed S species caused the passive film formed on Permalloy at the conclusion of RIE etching of the Ta and during subsequent exposure to air to poorly protect the Permalloy. If improper activation of the $Ni_{81}Fe_{19}$ surface occurred during RIE, then incomplete etching subsequently occurred in solution; the $Ni_{81}Fe_{19}$ underwent passivation rather than etching reactions.

Physical Characteristics of Etched Junctions

The magnetic behavior of MRAM elements is strongly dependent on shape anisotropy. Figure 5 shows top-down SEM micrographs of ion milled and wet etched Ta-capped MRAM elements. The latter were formed from sputter deposited films of the following type: Si | SiO_2 | Ta (100 Å) | $Ni_{81}Fe_{19}$ (50 Å) | Ta (100 Å). The ion milled junction (Fig. 5(b)) exhibits blunt points, and contains redeposited material, or "fences", represented by the white region at the element perimeter.

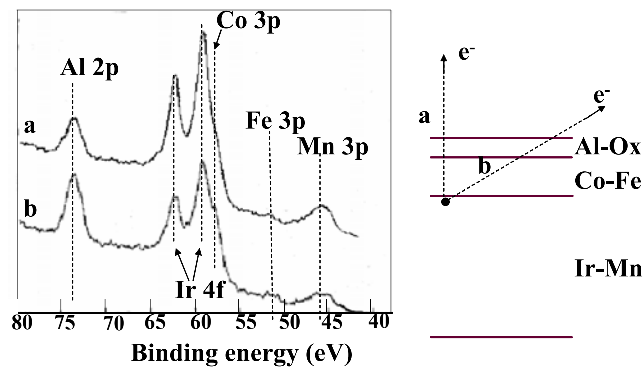

Figure 4. XPS spectra for MTJ stack following soft layer etching. Spectrum a) was recorded at a 90° angle, while b) was recorded at an angle < 90°.

The wet etched MRAM element (Fig. 5(a)) exhibits better shape characteristics than the ion milled element. This is a consequence of using a chemically efficient RIE process

to first pattern the Ta cap layer, and hence, no fence material is evident at the edges of the element.

A TEM image of a cross-section of part of an etched element is shown in Fig 6. In this case, a ternary alloy, $Ni_{65}Fe_{15}Co_{20}$, rather than Permalloy, was used as the magnetic layer. The top Ta layer was again patterned using RIE. The TEM image shows that little lateral etching occurred for the ternary alloy layer, which is visible in the image between the darker, higher-mass Ta layers. A passive oxide film is visible on the Ta mask, and also on the bottom Ta layer exposed on etching away the magnetic layer.

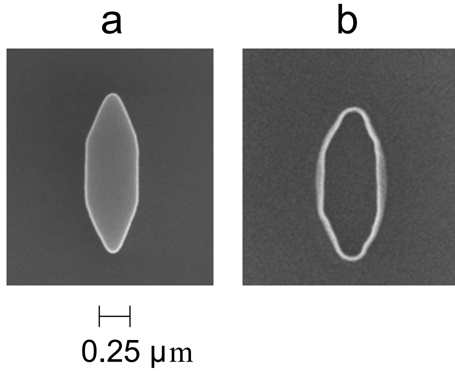

Figure 5. SEM images of a chemically-etched MRAM element (a) and an ion milled element (b).

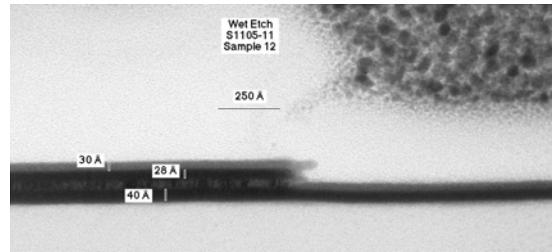

Figure 6. TEM cross-section of a chemically-etched MRAM element of the following type: Si | SiO_2 | Ta (40 Å) | $Ni_{65}Fe_{15}Co_{20}$ (50 Å) | Ta (40 Å).

<u>Magnetic Behavior</u>

A hysteresis loop, recorded using alternating gradient magnetrometry (AGM), is shown in Fig. 7 for an array of Permalloy elements. The data represent the average hysteresis behavior recorded for about 2 million elements (each 0.28 µm x 1.4 µm). This curve shows a mean coercivity (H_c) of 103 Oe, and a sharp, average transition characterized by a switching field standard deviation value σ of 3.7 Oe.

The ratio H_c/σ, or "array quality factor" (AQF), is an indicator of the quality of magnetic switching. The AQF value derived from the curve in Fig. 7 is ca. 28. As indicated earlier, an AQF value in excess of about 20 is needed in practical MRAM devices to avoid write failures. The results in Fig.

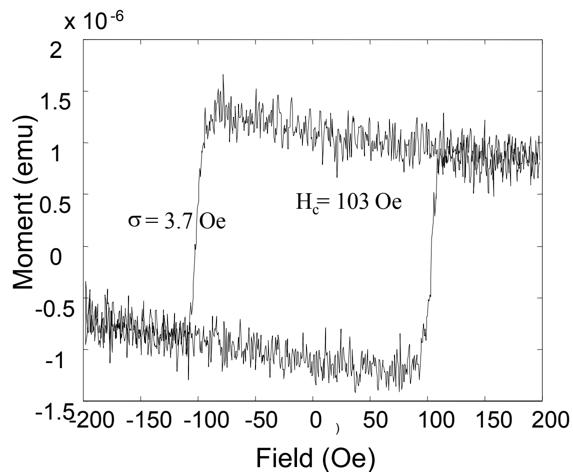

Figure 7. AGM hysteresis loop for a chemically etched array of magnetic elements made from the following thin film stack: Si | SiO_2 | Ta (50 Å) | $Ni_{81}Fe_{19}$ (50 Å) | Ta (50 Å). Etchant: 0.05 mol dm^{-3} suberic acid at pH = 5; time = 8.0 min.

7 indicate that chemical etching has promise for patterning MRAM magnetic layers.

Figure 8 shows switching field distribution data for a range of etch times for an array of Permalloy elements which were of size 0.28 µm x 1.4 µm. The AQF data displayed in Fig. 8(c), was obtained from the switching field data and spread data in Figs. 8(a) and 8(b), respectively. The AQF values increased with etch time, indicating that the magnetic switching properties of the array of elements improved with etch time, i.e., the range of switching fields exhibited by the array of elements tightened. To attempt to explain this result, it is worth discussing the data in Figs. 8(a) and (b).

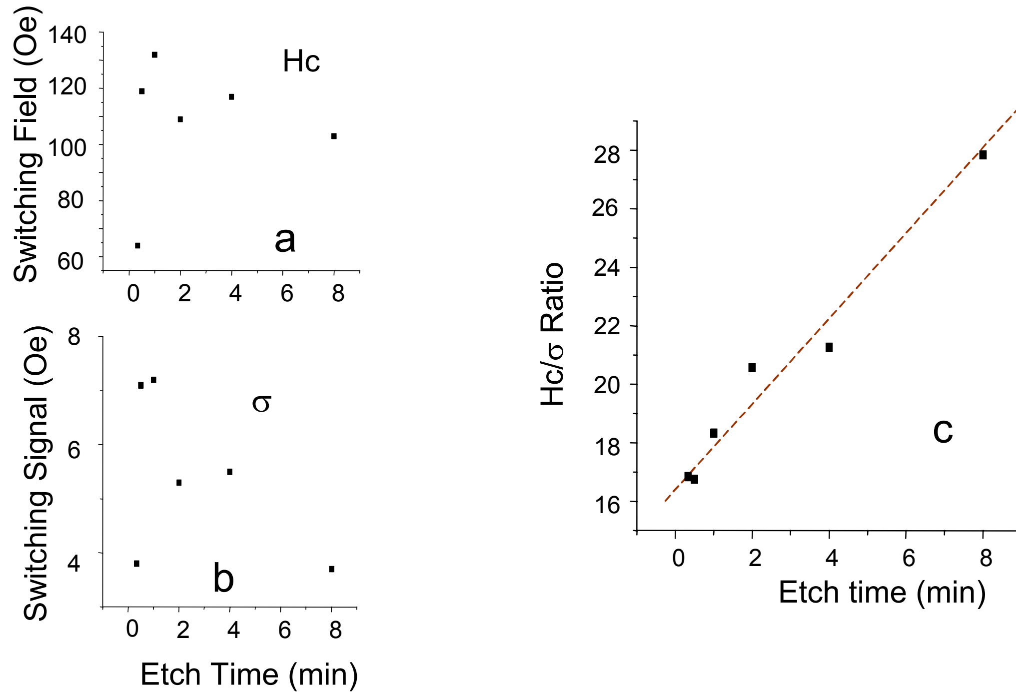

Figure 8. Array switching distribution behavior versus etch time. Data obtained using AGM method. Magnetic stack was of the following composition: Si substrate | SiO_2 | Ta (50 Å) | $Ni_{81}Fe_{19}$ (50 Å) | Ta (50 Å).

The switching field, or Hc, data in Fig. 8(a) shows a maximum at about one minute of etching time and then remains unchanged for longer etch times, or shows a gradual decrease. This is a surprising result, since one would expect Permalloy etching to continue and, as the diameter of the Permalloy elements decreased, Hc to increase. Either some unascertained change in the properties of the Permalloy elements occurred, such as in element aspect ratio, shape or magnetization, or a drastic decrease in, or ceasing of, Permalloy etching occurred at the element edges. Of significant interest is the fact that the switching field distribution actually tightened (Fig. 8(b)) with increase in etch time. This trend is somewhat surprising considering that for all of the etch times reported the inter-element regions of the films were completely etched, as indicated by the relatively constant switching field shown in Fig. 8(a). The further improvement in σ is likely due to improved TJ edge smoothness (due to preferential etching at remaining actives sites, including the two pointed regions of the Permalloy elements). Finally, the

increase in AQF with etch time at longer times was mainly driven by the decrease in the value of σ, and surprisingly was not helped by increasing values of Hc. For MRAM applications, increasing values of Hc with etch time would not be desirable, since higher write currents would have to be employed in MRAM devices to generate the appropriate switching fields.

Etching thin films of Permalloy (e.g. $\leqslant$ 100 Å thick) containing trace amounts of S additive chemisorbed on the surface (in this instance derived from the SF_6 RIE gas) is likely to proceed at a more rapid rate than etching bulk, or thick film, Permalloy. When etching thick-film Permalloy in a weak etchant, such as suberic acid solution at pH 4 – 5, competition may develop between dissolution into solution and growth of a passive film. The latter may drastically slow Permalloy element etching, since dissolution of the passive film is then relied upon to promote Permalloy etching. In the case of Permalloy, O_2 gas oxidant dissolved in solution may promote growth of a metastable passive film, which undergoes dissolution at a slow rate. In the limiting case of a passive oxide film inhibiting dissolution, Permalloy films which did not contain a Ta cap layer but which were exposed to air (oxygen plus humidity), did not undergo dissolution in the acid etchants employed in this work.

Figure 8(b) shows that the switching signal (σ) also exhibits a maximum at about one minute, and then decreases at longer etch times. A possible explanation for the trend in the data for σ is that Permalloy etching was incomplete at the shorter etch times, and that either a ragged profile, or device-to-device variations, contributed to greater switching non-uniformity. However, as etch time increased, the etching rate, i.e. at element edges, of initially-formed elements apparently slowed, and those elements which originally lagged in definition continued to be etched. Further smoothing of the edges would also be expected, thereby reducing switching field spread. It is possible that there was initial non-uniformity in the process of patterning the Permalloy elements since, a) a weak etchant was employed which would have initially etched more active regions of the Permalloy surface, and b) local, or pattern-dependent, non-uniformity may have been a feature of the preceding RIE step. In the case of the latter step, it is possible that trace amounts of Ta may have remained on regions of the Permalloy surface, and a non-uniform distribution of activating S additive on the Permalloy surface may also have resulted.

CONCLUSIONS

Chemical etching shows promise for selective patterning of magnetic soft (or free) layers, principally Permalloy, in MRAM stacks. Passive films formed in the prior cap layer patterning step play a critical role in the etching behavior of the magnetic layers. The novel use of a sulfur-based additive to inhibit Permalloy passivation, thus enabling selective etching in weak acid etchants, was demonstrated. Aqueous etch solutions of α, ω-dicarboxylic acids were found to etch Permalloy films whose surfaces contained a chemisorbed, sulfur-based, passivation inhibitor. The longer chain dicarboxylic acids, especially suberic, not alone etched Permalloy but left intact the alumina tunnel barrier and the underlying “pinned” magnetic layer. High values of array quality factors for magnetic switching were demonstrated for chemically etched arrays of Permalloy elements.

There is a need to continue developing an understanding of thin magnetic film chemical etching, especially in the context of MRAM to, a) help develop an understanding of corrosion issues that emerge in the relatively complicated MRAM stacks, and b) apply knowledge gained to the wet cleaning technology used after RIE etch patterning

ACKNOWLEDGEMENTS

The authors gratefully acknowledge S. Parkin, A. Gupta, and S. Brown for films; P. Rice (IBM Almaden) for TEM analysis; experimental help from B. Varghese and P. Bhatnagar; W. Gallagher and A Gupta for discussions and encouragement; DARPA for partial support of this work.

REFERENCES

1. W.J. Gallagher et al., *J. Appl. Phys.,* **81**, 3741 (1997).
2. B.N. Engel et al., *IEEE Trans. Nano.*, **1**, 32 (2002).
3. R.P. Cowburn, *Materials Today*, **July/August**, 32 (2003).
4. E.J. O'Sullivan and A. Schrott, *U.S. Patent* 6,426,012 (2002).